Journal of Physics:
Conference Series

PAPER • OPEN ACCESS

Forecast error mitigation for the ramp-constrained operation of wind farms

To cite this article: Jenna Iori *et al* 2026 *J. Phys.: Conf. Ser.* **3224** 032075

The Science of Making Torque from Wind (TORQUE 2026) IOP Publishing
Journal of Physics: Conference Series **3224** (2026) 032075 doi:10.1088/1742-6596/3224/3/032075

Forecast error mitigation for the ramp-constrained operation of wind farms

Jenna Iori[1], **Michiel Zaaijer**[1], **Dominic von Terzi**[1] **and Simon Watson**[1]

[1]Faculty of Aerospace Engineering, Delft University of Technology, the Netherlands

E-mail: j.iori@tudelft.nl

Abstract. Power ramp events represent an important challenge to grid stability, motivating the enforcement of ramp limits. For wind farm operation, decisions to respect these limits are based on imperfect forecast data, where errors can lead to deviations from the prescribed limit. In this study, we propose two different methods to mitigate the impact of forecast uncertainties on the operation of ramp-constrained wind farms: the use of a pessimistic forecast, where ramp events are worsened artificially, and the use of a storage system. The two methods are assessed by solving an online dispatch optimization problem for one year of operation. Forecast data are generated from numerical weather prediction models of the ECMWF. The dependence of power production on wind speed and direction changes is captured by an engineering wake deficit model. Results for 20 different offshore sites in Europe show that using a pessimistic forecast reduces the number of ramp events exceeding the limit by one third but increases curtailment by 0.2 percentage points on average. Instead, adding a storage system to the wind farm is more effective at reducing curtailment, proportionally to its size. The impact of forecast errors is mitigated most effectively by combining the two methods.

1. Introduction

The variability and uncertainty of wind power production pose important challenges in terms of grid stability and security of supply. In particular, ramp events, where the power production increases or decreases significantly in a short period of time, require the quick mobilisation of reserve capacity to balance the grid when they are not forecasted accurately. This issue has raised interest in enforcing a limit on the ramp rate for wind farms [1, 2].

For sudden increases in wind speed, this type of constraint can usually be satisfied by curtailing power reactively. However, for sudden decreases in wind speed, curtailment has to start before the event, to gradually reduce the power before it would drop. Thus, an accurate forecast is essential in order to plan curtailment sufficiently ahead of time to respect the limitation. While identification and forecasting methods for ramp events have been developed in the literature [1, 3, 4], uncertainties remain, raising the issue of managing their impact during operation.

One possible method for forecast error mitigation is the use of a storage system, co-located with the wind farm. While they are associated with a high capital expenditure, storage systems have shown their ability to mitigate forecast errors for wind farms participating in the electricity markets [5–7]. They are also promising to reduce curtailment by shifting the power delivery in time. Another approach, inspired by the field of chance-constrained optimization, is to use a pessimistic version of the forecast to encourage a more conservative operation. This method has

Journal of Physics: Conference Series **3224** (2026) 032075 doi:10.1088/1742-6596/3224/3/032075

been shown to mitigate the effect of forecast errors for the operation of baseload hybrid power plants, in a previous work by the authors [8].

In this study, the goal is to compare the effectiveness of the two aforementioned techniques, with the following research question: To what extent can curtailment and extreme ramp events be mitigated by the addition of a storage system or the use of a pessimistic forecast, for ramp-constrained operation of wind farms?

In the following sections, the index j refers to the time step and i the forecast lead-time. We use standard font for scalars ($\hat{P}_i^d$) and bold font for vectors ($\hat{\boldsymbol{P}}^d$). Forecasted and estimated values are indicated by a circumflex ($\hat{\square}$), and optimal values by an asterisk ($\square^*$).

2. Dispatch optimization problem

In order to respect a given power ramp constraint, a wind farm operator needs to decide when to curtail energy and at which magnitude. In this work, these decisions, referred to as dispatch strategy, are supported by a series of optimization problems solved at every time step with updated forecast information. At a given time step j, an optimization problem is formulated to estimate the delivered power $\hat{\boldsymbol{P}}^d$ for the next n steps, based on the power production forecast issued at time j, $\hat{\boldsymbol{P}}^w_{|j}$. The goal of the optimization problem is to maximize the amount of energy delivered for the n steps ahead, while limiting the magnitude of the power ramp below a threshold δP_{lim}. In addition, the delivered power is bounded by the rated power of the wind farm, P_{max}. Once the problem is solved, the power is delivered following the optimum for one time step, i.e, $P_j^d = \hat{P}_0^{d*}$, and the process is iterated as illustrated in Figure 1.

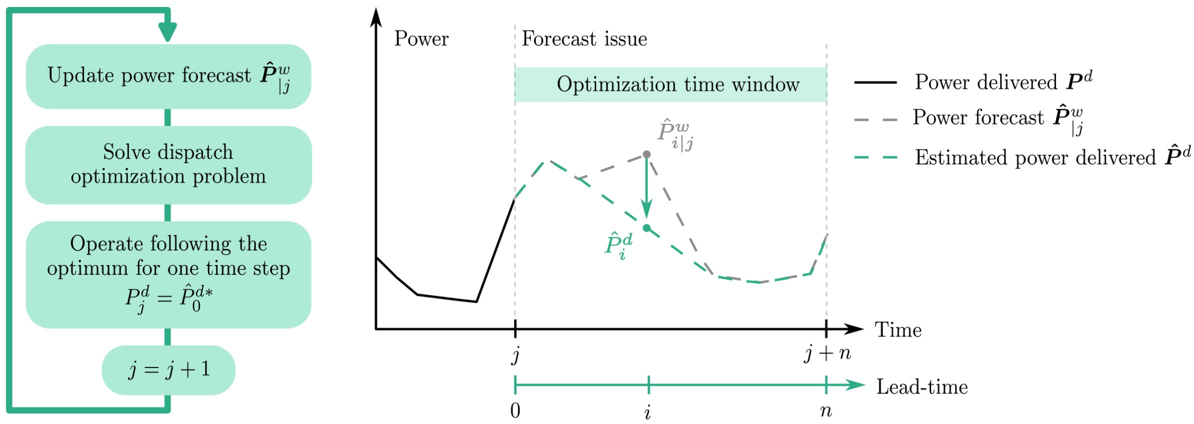

Figure 1. Illustration of the dispatch optimization process

It has been chosen to formulate the optimization problem in a form suitable for mixed integer linear programming. The system and component behaviour is modelled in the form of linear constraints on the design variables, which include binary variables, as described below. Special attention is required for the formulation of the power ramp limit. In some cases, this constraint may be unfeasible, e.g., because errors in the power forecast have left the farm in an unfavourable state at the previous time step. To address this, the ramp constraint is relaxed. We use (i) a penalty term p for the ramp constraint at lead-time $i = 0$, (ii) binary variables $\boldsymbol{z}$ representing the enforcement of the ramp constraint, and (iii) a reliability penalty r on the binary variables. This results in the following optimization constraints,

Journal of Physics: Conference Series **3224** (2026) 032075 doi:10.1088/1742-6596/3224/3/032075

$$
\begin{aligned}
0 \leq & \hat{P}_i^d \leq P_{\max}, & i = 0, .., n-1 \quad (1)\\
-\delta P_{\lim} - p \leq & \hat{P}_0^d - P_{j-1}^d \leq \delta P_{\lim} + p, & (2)\\
-P_{\max} - z_i(\delta P_{\lim} - P_{\max}) \leq & \hat{P}_{i+1}^d - \hat{P}_i^d \leq P_{\max} + z_i(\delta P_{\lim} - P_{\max}), & i = 0, .., n-2, \quad (3)\\
\sum_{i=0}^{n-2} z_i = & (n-1)(1-r). & (4)
\end{aligned}
$$

Then, if both r and p are equal to zero, the ramp constraint is satisfied for all lead-times. The objective function f is formulated to maximize the energy delivered and minimizing both penalty terms r and p, with tuning factors μ and λ, as

$$
f(\hat{\boldsymbol{P}}^d, p, r) = \sum_{i=0}^{n-1} (\hat{P}_i^d - \hat{P}_{i|j}^w) - \mu p - \lambda r. \quad (5)
$$

For the stand-alone wind farm, the dispatch strategy is represented by the curtailed power $\hat{\boldsymbol{P}}^c$, set to be positive. The delivered power $\hat{\boldsymbol{P}}^d$ is obtained by subtracting the curtailed power from the power forecast $\hat{\boldsymbol{P}}_{|j}^w$. This results in the following two constraints

$$
\begin{aligned}
\hat{P}_i^d = & \hat{P}_{i|j}^w - \hat{P}_i^c, & i = 0, ..., n-1, \quad (6)\\
\hat{P}_i^c \geq & 0, & i = 0, ..., n-1. \quad (7)
\end{aligned}
$$

Instead, when a storage system is added to the wind farm, the dispatch strategy includes the storage dispatch in addition to curtailment. The delivered power then depends on the storage power $\hat{\boldsymbol{P}}^s$, where $\hat{P}_i{}^s \geq 0$ in discharge, following

$$
\hat{P}_i^d = \hat{P}_{i|j}^w + \hat{P}_i^s - \hat{P}_i^c, \quad i = 0, ..., n-1, \quad (8)
$$

The storage energy level $\hat{\boldsymbol{E}}^s$ is calculated using the round-trip efficiency η, as

$$
\hat{E}_{i+1}^s - \hat{E}_i^s = \begin{cases} -\Delta t \hat{P}_i^s & \text{if } \hat{P}_i^s \leq 0, \\ -\dfrac{\Delta t}{\eta} \hat{P}_i^s & \text{else,} \end{cases} \qquad i = 0, ..., n-1, \quad (9)
$$

The power and energy levels are bounded using the values of the power capacity $\bar{P}^s$ and the duration d^s of the storage. Furthermore, the energy level at lead time $i = 0$ is enforced to equal the realized energy level, from the operation at the previous time step. Mathematically, the constraints related to the storage system are expressed as follows

$$
\begin{aligned}
\hat{E}_0^s = & E_j^s & (10)\\
0 \leq & \hat{E}_i^s \leq \bar{P}^s d^s & i = 0, ..., n-1, \quad (11)\\
-\bar{P}^s \leq & \hat{P}_i^s \leq \bar{P}^s & i = 0, ..., n-1, \quad (12)\\
\hat{E}_{i+1}^s - \hat{E}_i^s \leq & -\Delta t \hat{P}_i^s & i = 0, ..., n-1, \quad (13)\\
\hat{E}_{i+1}^s - \hat{E}_i^s \leq & -\frac{\Delta t}{\eta} \hat{P}_i^s & i = 0, ..., n-1, \quad (14)
\end{aligned}
$$

Here, we use a relaxed form of Eq. (9) to represent the storage model. This formulation choice allows the number of binary variables to be reduced and with it the computational cost of solving the problem. However, it requires the addition of two regularization terms to the objective function on the curtailed power and on the energy level of the storage system at the end of the optimisation window. The relaxation holds for all numerical experiments presented in this work.

The two optimization problems solved in this work are reported below. Eq. (15) represents the problem for the stand-alone wind farm and Eq. (16) the one when a storage system is added, with β the regularization factor. Since both problems are mixed-integer linear programs, they can be solved efficiently with off-the-shelf solvers.

$$\begin{aligned} \min_{\hat{\boldsymbol{P}}^c, \boldsymbol{z}, p, r} \quad & f(\hat{\boldsymbol{P}}^d, p, r) \\ \text{with} \quad & \text{Eq. (6)} \\ \text{s.t.} \quad & \text{Eqs. (1-4) and (7)} \end{aligned} \tag{15}$$

$$\begin{aligned} \min_{\hat{\boldsymbol{P}}^c, \hat{\boldsymbol{E}}^s, \hat{\boldsymbol{P}}^s, \boldsymbol{z}, p, r} \quad & f(\hat{\boldsymbol{P}}^d, p, r) + \beta E_n + \epsilon \sum_{i=0}^{n-1} \hat{P}_i^c \\ \text{with} \quad & \text{Eq. (8)} \\ \text{s.t.} \quad & \text{Eqs. (1-4), (7) and (10-14)} \end{aligned} \tag{16}$$

2.1. Robust dispatch using pessimistic forecast

The optimization problems represented by Eq. (15) and (16) use forecast data, but do not take into account the potential errors in this input. In order to mitigate the impact of forecast uncertainties, a pessimistic version of the forecast is built, where the wind speed ramp is assumed to have a higher magnitude than in the original forecast. Let $\hat{u}_{i|j}$ be the wind power forecast for a lead time i issued at time j. The pessimistic forecast, noted $\hat{u}^-_{i|j}$, is obtained by adjusting the magnitude of the ramp in the original forecast value by a factor α:

$$\hat{u}^-_{i|j} = \hat{u}^-_{i-1|j} + (1+\alpha)(\hat{u}_{i|j} - \hat{u}_{i-1|j}), \ \forall i > 1, j, \tag{17}$$

with $\hat{u}^-_{0|j} = \hat{u}_{0|j}$. An example of a pessimistic forecast is given in Figure 4, for the default value of $\alpha = 0.1$. The value of the parameter is chosen based on the standard deviation of the error of the wind speed ramp forecast. Thus, solving the dispatch optimization problems with the pessimistic forecast results in a more conservative dispatch strategy, based on forecast data where ramp events are magnified.

3. Wind farm power modelling

The power production of the wind farm is calculated from a look-up table of normalized power production. The look-up table is generated by simulating and normalizing the power production of a generic wind farm for discretized values of wind speeds and directions, with step sizes of 0.5 m/s and 2.5 ^{o}. We use the regular layout of the IEA 740-10-MW reference offshore wind plant [9] and the Bastankhah wake deficit model [10] implemented in PyWake [11], with a wake expansion factor of 0.05. Then, for a given wind speed and direction, the values in the look-up table are linearly interpolated and multiplied by the rated power of the wind farm $P_{\max}$ to obtain the wind farm power. This model captures the dependency of the power production to wind speed and direction changes, and thus the associated power ramp events. Figures 2 and 3 report the normalized power curve used in this work.

The power forecast is generated from the numerical weather prediction of the ECMWF's integrated forecast system, combining simulations and meteorological measurements. Specifically, we use the reanalysis historical forecast (hindcast) of the u and v wind speed components at 100 m. From this database, we retrieve a forecast issue every 12 hours and for lead-times with a varying resolution, between one hour (for lead-times up to 12 h), two hours (for lead-time between 12 and 24 h) and three hours (for lead-time above 24 h). The data are interpolated

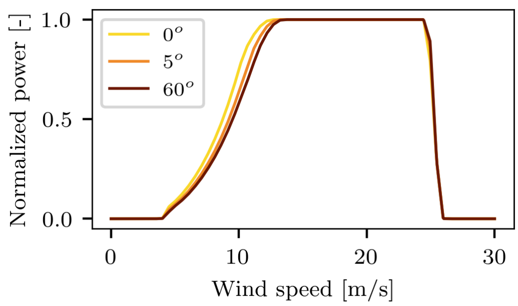

Figure 2. Normalized wind farm power curve as a function of the wind speed and for wind directions of 0^o, 5^o, and 60^o.

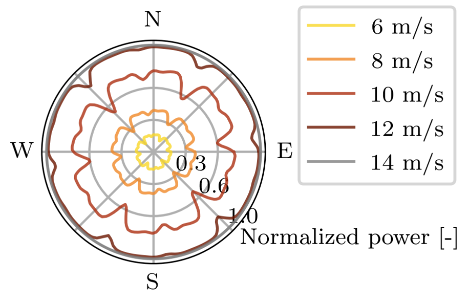

Figure 3. Normalized wind farm power curve as a function of the wind direction.

to obtain an hourly signal. Since numerical weather prediction (NWP) models tend to perform poorly for short lead times [12], the forecast is artificially improved for lead-times up to six hours. For this, we use a linear combination of observation data and NWP data, so that the forecast is equal to the observation for a zero hour lead time and equal to the NWP forecast for a six hour lead time. The observation data are obtain from ERA5 [13], specifically the hourly u and v components of the wind speed at 100 m. Both the observation and forecasted data are corrected to a wind turbine hub height of 119 m, using a shear coefficient of 0.09.

The ECMWF's integrated forecast system provides state-of-the-art data that is considered representative for the quality of forecast data available to wind farm operators. When forecasts with lower uncertainty are available, the performance with real information improves and less pessimism is needed. This can be achieved by tuning the pessimism coefficient to a lower value.

4. Numerical experiments

To answer the research question, numerical experiments are conducted to compare the use of a pessimistic forecast, a storage system or both for the operation of ramp-constrained wind farms. The dispatch optimization problems described in Section 2 are solved with a real-information (RI) or pessimistic (P) forecast generated with $\alpha = 0.1$. We consider a 100 MW wind farm required to respect a ramp-limit of 20 MW/h, with and without a 10 MW storage system (S) with 2 hours duration and a round trip efficiency $\eta = 0.85$. The problem is also solved with a perfect-information (PI) forecast, in order to assess the impact of forecast errors. This results in five different cases, listed in Table 1.

Table 1. Description of the case studies.

Case	Forecast input	Storage system capacity	Optimization problem
PI	Perfect Information	None	Eq. (15)
RI	Real Information	None	Eq. (15)
RI+S	Real Information	10 MW - 2 h	Eq. (16)
P	Pessimistic	None	Eq. (15)
P+S	Pessimistic	10 MW - 2 h	Eq. (16)

Journal of Physics: Conference Series **3224** (2026) 032075 doi:10.1088/1742-6596/3224/3/032075

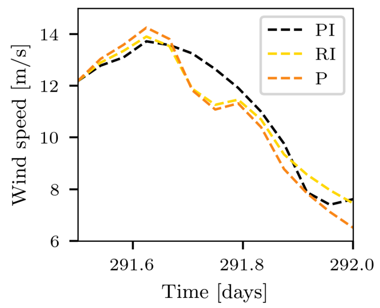

Figure 4. Example of perfect (PI), real information (RI) and pessimistic (P) wind speed forecasts for a period of 10 hours.

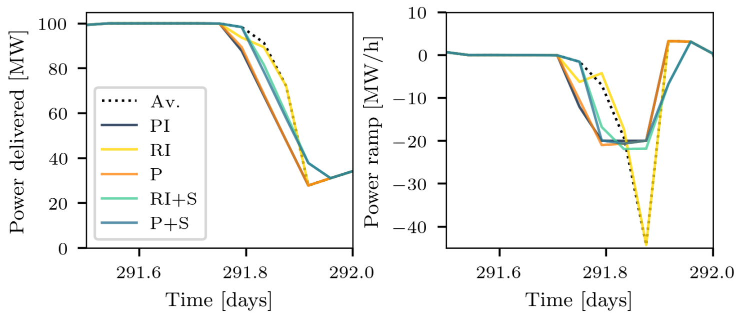

Figure 5. Power delivered and ramp rate for the dispatch calculated with PI, RI, and pessimistic (P) forecasts, and with or without a storage system. The available power (Av.) is marked in black dotted line.

In order to generalize our results, 20 different offshore sites in Europe are considered, reported in Figure 7. For each location, forecast and observation data are extracted and a power forecast signal is generated, using the method described in Section 3. Thus, we use the same wind farm layout and look-up table for all sites. While the power production is not maximized per location, this model is sufficient in capturing the power ramps due to wind speed and direction changes.

All data are extracted for the year 2019 and the dispatch strategy is simulated for approximately one year, with $\Delta t = 1$ hour and 8600 time steps. We consider a maximum lead time $n = 48$ hours. The optimization problem is implemented in the open-source code SHIPP [14] and solved with the interior-point method of MOSEK [15], with $\mu = \lambda = 100$, and $\beta = \epsilon = 10^{-6}$.

5. Results

5.1. Reference site

Results are first presented for the reference site, shown in Figure 7. Figure 5 reports the delivered power and corresponding ramp rate around a ramp event where the available power sees a ramp of -44 MW/h. The dispatch calculated with the Real Information (RI) forecast follows closely the ideal dispatch calculated with the PI forecast, but fails to respect the ramp constraint of 20 MW/h. Instead, with the pessimistic forecast, power is curtailed earlier, and the ramp limit is respected. Furthermore, with a storage system, the ramp limit is respected by discharging the storage, with the delivered power above the available one during the last part of the event.

Figure 6 reports the distribution of extreme ramp events for the different cases listed in Table 1. Only the down-ramps are reported, since the up-ramp limit is respected in all cases. For the RI forecast, there are 98 events violating the ramp limit. Using a pessimistic forecast, this number decreases to 57. Adding a storage system further reduces the number of extreme events, but still shows a similar trend between the RI and pessimistic forecasts, with 65 and 19 extreme events, respectively. The curtailment significantly varies depending on the presence of the storage system. Results show that the curtailed energy drops from around 1% to 0.3% when adding a storage system. Indeed, having storage capacity allows some of the otherwise curtailed energy to be stored when limiting the ramp rate. Instead, using a pessimistic forecast tends to increase curtailment, with or without the storage system. This is because it encourages a conservative dispatch operation, where the power is curtailed earlier and thus often at a larger magnitude.

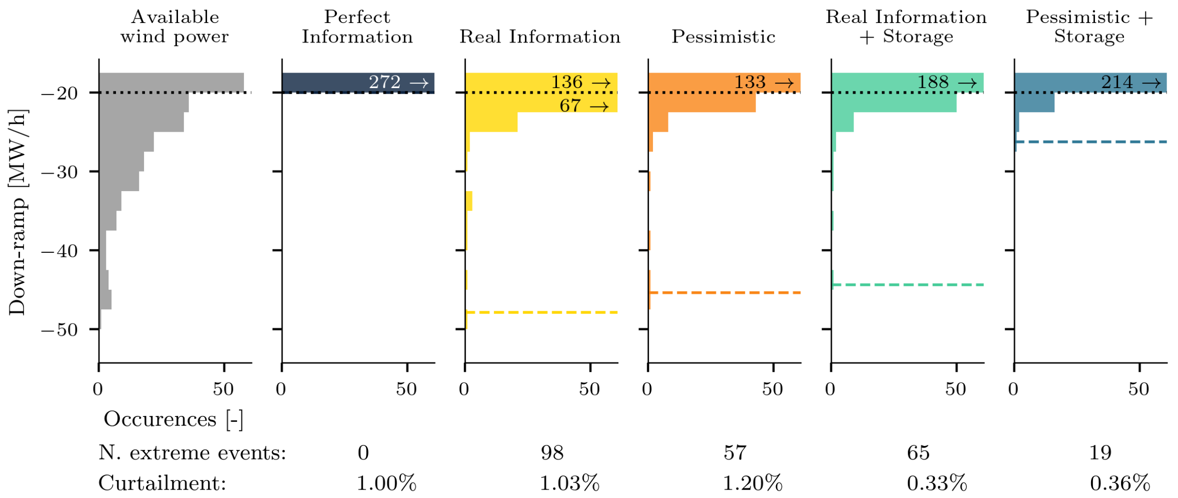

Figure 6. Distribution of ramp rates around and below the limit of -20 MW/h for a dispatch calculated with different forecasts, and without or with a storage system, with the ramp rate of available power reported as a reference in the leftmost plot. The dashed line represents the magnitude of the worst ramp.

5.2. *All sites*

The analysis is repeated for 19 additional sites. Figure 8 reports the curtailment and the number of events violating the ramp limit for all sites, and for the different cases listed in Table 1. The data confirm the trends identified for the reference site. First, the use of a pessimistic forecast decreases the number of extreme events by one third on average, while increasing the curtailment by around 0.2 percentage points, compared to the RI case. Furthermore, the addition of a storage system decreases the curtailment by 0.7 percentage points, with a similar decreases in the number of extreme events. The combination of the two methods is most effective, with an

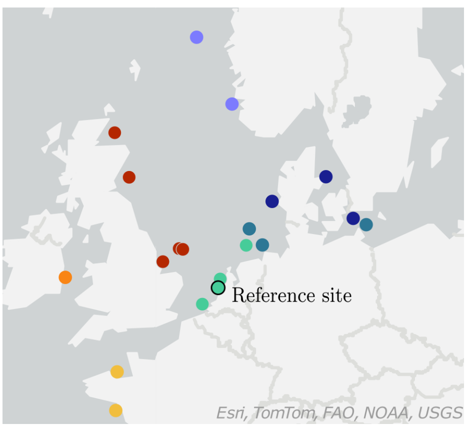

Figure 7. Locations of the 20 offshore wind farm sites. The reference site is represented with a black circle.

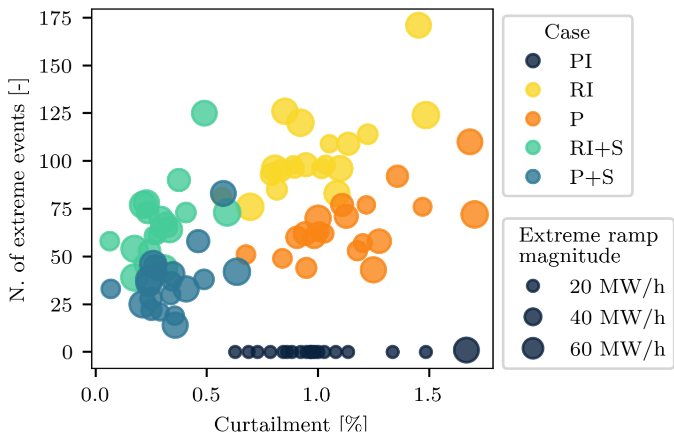

Figure 8. Curtailment and number of extreme events for 20 sites and for perfect information (PI), real information (RI) and pessimistic (P) forecasts, without or with storage (S). The marker size indicates the magnitude of the worst ramp.

Journal of Physics: Conference Series **3224** (2026) 032075 doi:10.1088/1742-6596/3224/3/032075

average curtailment of 0.3% and a 64% decrease in the number of extreme events. We note that for one site, the ramp limit is exceeded even with perfect information. This is because one large ramp event occurs during the second hour of the simulation, and cannot be mitigated.

In terms of the maximum ramp magnitude, the trend identified for the reference site is more difficult to generalize. Figure 9 reports the impact of the use of a pessimistic forecast on the distribution of the worst ramp events across sites. Data show that on average, the magnitude of the worst ramp event decreases with the use of a pessimistic forecast, and with the use of a storage system. This is particularly visible for ramp events between -90 and -100 MW/h. With a RI forecast, seven sites see a ramp with this magnitude. The number decreases to three for the use of a pessimistic forecast, two with a storage system and zero when both approaches are used. However, for some sites, the magnitude of the largest ramp increases with the use of a pessimistic forecast (two sites), a storage system (three sites) or both (four sites).

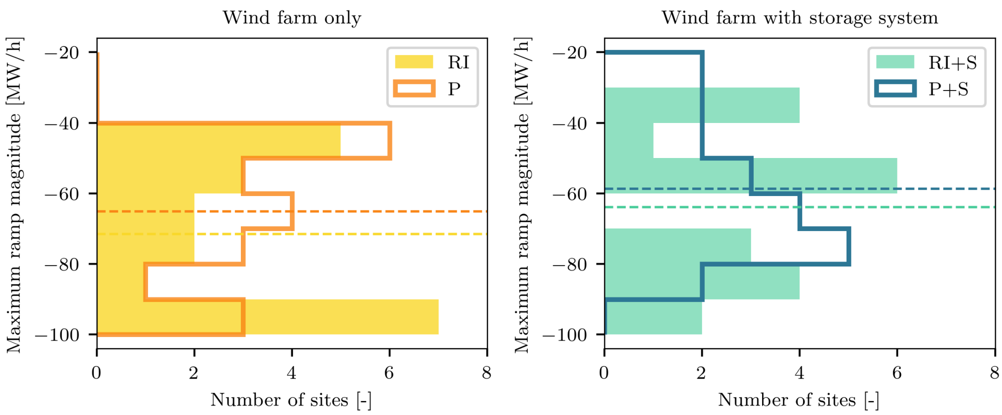

Figure 9. Distribution of the magnitude of the worst ramp event for the 20 site locations, and considering a real-information (RI) or pessimistic (P) forecast, with and without a storage system (S). The average over all sites is represented by a dashed line.

We note that the magnitude of extreme ramp events was found to be sensitive to the choice of wake model, whereas the trends identified previously for curtailment and number of extreme events were unaffected. Thus, the wind farm model should be carefully chosen and calibrated to analyse extreme ramp events.

5.3. Sensitivity analysis

To get a better understanding of the presented results, a sensitivity analysis is conducted on the value of the pessimism factor α and on the storage size, for the reference site.

Figure 10 shows that when increasing the parameter α, the number of extreme events reduces at the cost of increased curtailment, showing a trade-off between the two metrics. When adding a storage system, curtailment shows a smaller increase, since the storage system allows the operator to store energy instead of curtailing it. However, increasing α shows diminishing returns on the mitigation of extreme ramp events, with and without storage. Consequently, the value of α should be based on relative value of curtailing energy compared to a violation of the ramp limit. Furthermore, the value of α depends on the characteristics of the forecast data. We suggest using a value of α with the same order of magnitude as the standard deviation of the forecast error. In this study, α is chosen based on an analysis of the forecast data. The standard deviation of the forecast error for wind speed ramps was found to be between 6 and 12 % of the mean wind speed per hour across sites, and lead to the default value of $\alpha = 0.1$.

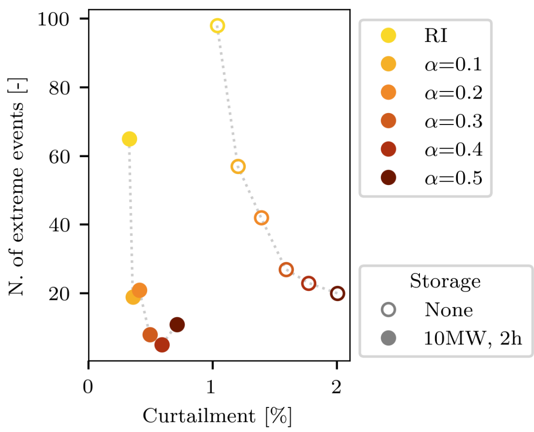

Figure 10. Impact of the pessimism factor on the number of extreme ramp events and curtailment, with and without storage system

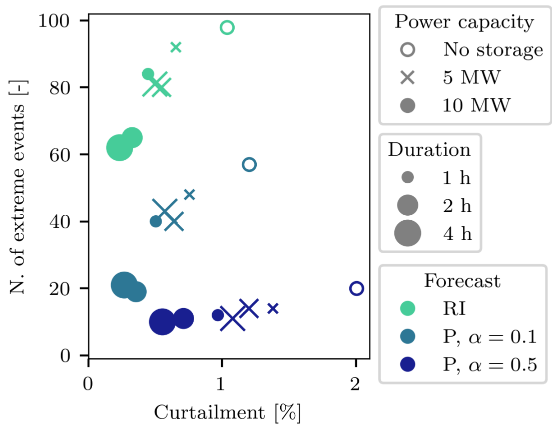

Figure 11. Impact of the storage power capacity and duration on the number of extreme ramp events and curtailment, considering a real information forecast (RI) or its pessimistic version

Figure 11 reports the number of extreme events and curtailment for storage durations of 1, 2, and 4 hours and a power capacity of 5 and 10 MW. For completeness, the numerical experiments are also run for a pessimistic forecast with $\alpha = 0.1$ and $\alpha = 0.5$. Results show that curtailment reduces with an increase in storage size. The number of extreme events is also reduced, but with a lower magnitude the higher the pessimism factor. These results suggest that the storage system is mainly effective at reducing curtailment. While the pessimistic forecast allows a reduction of the number of extreme event, a small storage system can instead mitigate the associated increase in curtailment. A parametric study across storage sizes would allow allow an estimate of the adequate storage design to improve the effectiveness of ramp limitation.

6. Limitations and Discussion

In this work, the generation of the pessimistic forecast is based on a simple reformulation of the input wind speed, where the ramp rate at each time step is worsened by a given factor. This means that small wind speed variations due to turbulence are not distinguished from larger and low-frequency events. Furthermore, this approach does not account for ramp events caused by changes in wind speed direction. We expect that a more detailed method to generate the pessimistic ramp forecast, e.g., using advanced ramp event identification methods, will lead to better results.

Furthermore, the model used to simulate the behaviour of the storage system does not take into account battery degradation, variable electricity price, or variable availability of the wind farm or storage system. These aspects would be relevant to an operator using the methodology, since they would affect the optimal operation. Adjustments could be made to the optimization problem to include them. However, we expect that the results for the different forecast signals would be similarly affected. For the proof of principle of the methodology this study is focused on the trends, which we therefore expect to be less affected by this omission. Likewise, the pessimistic forecast approach can be extended to consider shutdowns of the power plant components by implementing a forecast of their remaining useful life.

Due to the large capital cost generally associated with storage systems, a complete techno-

Journal of Physics: Conference Series **3224** (2026) 032075 doi:10.1088/1742-6596/3224/3/032075

economic analysis is necessary to determine if the addition of a storage system is beneficial beyond the ramp limitation studied here. Our results show that adding a 10 MW and 2-hour duration storage system reduces curtailment by 0.7 to 1.3 percentage points. Using data from the Danish Energy Agency [16, 17], the cost of this storage for 2030 represents 2% of the capital expenditure of a 100 MW bottom-fixed offshore wind farm. This added capital expenditure can potentially be offset by the reduction in curtailment. However, analysing the trade-off between added costs and avoided curtailment relies on several assumptions, e.g. the number of battery replacements during the project lifetime, expected number of hours when ramp-limitation is enforced, and electricity price during periods of curtailment, and thus requires an in-depth and dedicated study.

7. Conclusion

This study compares two methods to mitigate forecast errors when limiting the power ramp rate of wind farms: the use of a pessimistic power forecast and the addition of a storage system. The dispatch strategy of the wind farm is calculated based on a dispatch optimization problem solved every time step, considering a standard forecast or its pessimistic version, and with or without a storage system. An analysis over 20 offshore wind farm sites in Europe shows a reduction of extreme ramp events by one third on average using the pessimistic forecast at the cost of an increase in curtailment. The use of a storage system reduces the number of extreme event by a similar magnitude, but additionally leads to a notable decrease in curtailment. The best performance is obtained by combining the two approaches, with an 64% reduction of the number of extreme ramp events. Our study demonstrates that the number of extreme events can be further reduced by making the forecast more pessimistic or increasing the storage size, at the expense of increased curtailment and storage system costs, respectively.

Overall, this work indicates that the impact of forecast errors can be mitigated effectively, leading to better management of curtailment in wind farms and a reduction of extreme ramp events detrimental to grid stability. With this knowledge, wind farm developers and operators can compare and select the most suitable mitigation strategy for their specific conditions. In turn, policy makers and transmission system operators can assess the impact of delegating ramp-event mitigation to power-producing assets, thereby supporting more effective integration of wind energy in the broader energy system.

Code and data availability

All results presented in this study can be reproduced using the published data [18] and code available at github.com/jennaiori/torque26-128 [19], based on the open-souce code SHIPP [14].

Acknowledgements

The results presented in this study are based on data from the European Centre for Medium-Range Weather Forecasts (ECMWF). This work is part of the Hollandse Kust Noord wind farm innovation program on system integration. Funding was provided by CrossWind C.V., and content support was provided by Shell and Eneco. In addition, sincere thanks are addressed to two reviewers for their comments and suggestions that helped raise the quality of this article.

Journal of Physics: Conference Series **3224** (2026) 032075 doi:10.1088/1742-6596/3224/3/032075

References

[1] Jia Y, Ren B, Li Q, Wang C, Wang D and Zou X 2023 An Integrated Scheme for Forecasting and Controlling Ramps in Offshore Wind Farms Considering Wind Power Uncertainties during Extreme Storms *Electronics* **12** 4443

[2] D'Amico G, Petroni F and Vergine S 2022 Ramp Rate Limitation of Wind Power: An Overview *Energies* **15** 5850

[3] Muschinski T, Lang M N, Mayr G J, Messner J W, Zeileis A and Simon T 2022 Predicting power ramps from joint distributions of future wind speeds *Wind Energ. Sci.* **7** 2393–2405

[4] Cheneka B R, Watson S J and Basu S 2020 A simple methodology to detect and quantify wind power ramps *Wind Energ. Sci.* **5** 1731–1741

[5] Ding H, Pinson P, Hu Z and Song Y 2016 Integrated Bidding and Operating Strategies for Wind-Storage Systems *IEEE Transactions on Sustainable Energy* **7** 163–172

[6] Luo F, Meng K, Dong Z Y, Zheng Y, Chen Y and Wong K P 2015 Coordinated Operational Planning for Wind Farm With Battery Energy Storage System *IEEE Transactions on Sustainable Energy* **6** 253–262

[7] Das K, Philippe Grapperon A L T, Sørensen P E and Hansen A D 2020 Optimal battery operation for revenue maximization of wind-storage hybrid power plant *Electric Power Systems Research* **189**

[8] Iori J, Zaaijer M, Kreeft J, Terzi D V and Watson S 2025 Reliable operation of wind-storage systems for baseload power production *J. Phys.: Conf. Ser.* **3025** 012023

[9] Kainz S, Quick J, Souza de Alencar M, Moreno S, Dykes K, Bay C, Zaaijer M and Bortolotti P 2024 *IEA Wind TCP Task 55: The IEA Wind 740-10-MW Reference Offshore Wind Plants* (IEA)

[10] Bastankhah M and Porté-Agel F 2014 A new analytical model for wind-turbine wakes *Renewable Energy* **70** 116–123

[11] Pedersen M M, Forsting A M, van der Laan P, Riva R, Alcayaga Romàn L A, Criado Risco J, Friis-Møller M, Quick J, Schøler Christiansen J P, Valotta Rodrigues R, Olsen B T and Réthoré P E 2023 PyWake 2.5.0: An open-source wind farm simulation tool Publisher: DTU Wind, Technical University of Denmark

[12] Giebel G, Brownsword R, Kariniotakis G, Denhard M and Draxl C 2011 The State-Of-The-Art in Short-Term Prediction of Wind Power: A Literature Overview, 2nd edition Tech. rep. ANEMOS.plus

[13] Hersbach H, Bell B, Berrisford P, Hirahara S, Horányi A, Muñoz-Sabater J, Nicolas J, Peubey C, Radu R, Schepers D and others 2017 Complete ERA5 from 1940: Fifth generation of ECMWF atmospheric reanalyses of the global climate *Copernicus Climate Change Service (C3S) Data Store (CDS)* **10**

[14] Iori J 2025 Shipp - a design optimization software for hybrid power plants URL `https://github.com/jennaiori/shipp`

[15] MOSEK ApS 2024 *The MOSEK Optimizer API for Python 10.2.0* URL `https://docs.mosek.com/latest/pythonapi/index.html`

[16] Danish Energy Agency 2025 *Energy storage: technology descriptions and projections for long-tem energy system planning* (Danish Energy Agency)

[17] Danish Energy Agency 2025 *Generation of electricity and district heating: technology descriptions and projections for long-tem energy system planning* (Danish Energy Agency)

[18] Iori J 2026 Data associated with the publication "Forecast error mitigation for the ramp-constrained operation of wind farms"

[19] Iori J 2026 Code associated with the publication "Forecast error mitigation for the ramp-constrained operation of wind farms"